EE412 Spring 2014 Project

SiN_x PECVD and Nanostructure Etching Recipe Development

Yusi Chen and Muyu Xue

SNF Mentor: Jim McVittie

Faculty Mentor: James Harris

I. Introduction

Amorphous materials deposited using PECVD, including SiN_x, α-Si and SiO_2, have a variety of applications in both electronics and photonics. They can be used for surface passivation [1], anti-reflection [2], strain layer [3], heterostructures [4] and many other aspects. In order to achieve these applications, the properties of the materials, including refractive index, energy bandgap, material composition, strain, and etc., need to be optimized with careful PECVD recipe development. However, in SNF, such recipes are not widely available for our PECVD tools, including STS, CCP and HDPECVD. At the same time, in order to use those materials in different applications, optimized dry etching and wet etching recipes with regard to different materials are also needed.

In this project, we will focus on the development of deposition and corresponding etching recipes for PECVD SiN_x [5-7]. First, we will focus on high stress PECVD SiN_x for photonics application using CCP and STS. Second, we would like to try to form nanostructures and photonic structures on the SiN_x films using isotropic dry etching technology in PT-OX [8]. Such recipes will be updated on the SNF wiki and will benefit the whole research community of SNF.

II. High stress PECVD SiN_x recipe development

a. SiN_x Deposition Stress State Characterization

To test the stress state on the SiN_x stressor layer by Plasma-Enhanced Chemical Vapor Deposition, the experiments are performed on two PECVD tools in SNF: CCP PECVD and STS PECVD, respectively.

For the CCP PECVD, a systematical study is conducted for the stress range can be achieved by this tool. There are for steps in each SiN_x recipe: thermal soak, gas stabilization, deposition and N_2 flush. We only change the parameters for gas stabilization and deposition process. The deposition temperature is kept constant at 350℃ and the chamber pressure is kept at 950mTorr (All the parameter details for thermal soak and N_2 flush is included in the appendix). The controlled variables include the ratio of NH_3/SiH_4, and the percentage of N_2 in mixture of N_2 and helium. The whole range of stress state can be achieved by CCP and characterization of the uniformity is concluded.

For the STS PECVD, due to its good performance for large compressive stress and excellent uniformity, the compressive stress experiment is designed to achieve large compressive stress. The temperature is kept constant at 350℃, the controlled variables include chamber pressure, the ratio of NH_3/SiH_4, deposition time, process power. Because STS PECVD does not include helium during the deposition, this potential variable is not included in this set of experiments.

b. Stress Test Results

i. CCP PECVD

The experiments are conducted on three subsets according to the percentage of N_2 in mixture of N_2 and helium. Based on stress determining physics, the higher percentage of N_2 in the mixture, the stress in the SiN_x moves more to the tensile side. Thus this percentage is kept in three values: $N_2/(N_2+He)=0$ (compressive limit), $N_2/(N_2+He)=60\%$ (intermediate case) and $N_2/(N_2+He)=80\%$ (tensile limit).

1. Tensile stress limit:

N_2 /(N_2+He)=80%, the N_2 flow is kept at 800sccm and He flow is kept at 200sccm. Temperature is kept at 350℃ and the chamber pressure is kept at 950mTorr. Only the ratio of NH_3/SiH_4 is changed from 0.6 to 1.5. The stress of the experiments is shown in figure 1.

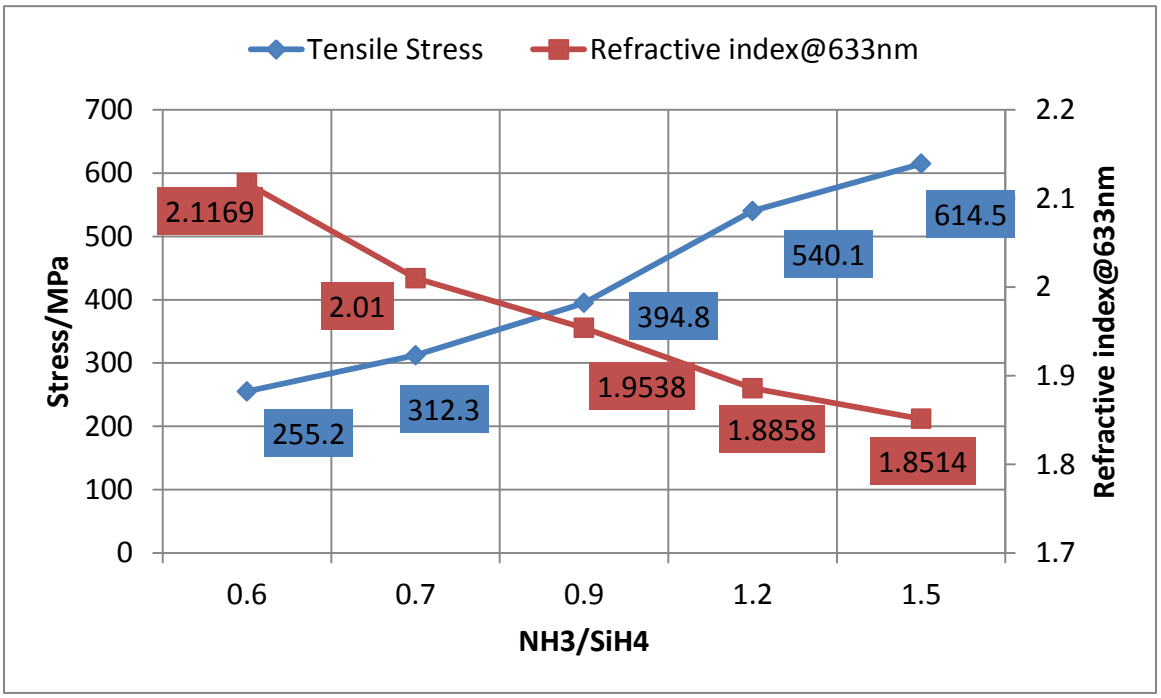

Figure 1 SiN_x Stress in tensile limit

Figure 1 shows that the stress in SiN_x in the tensile limit case is always tensile and gradually increases as NH_3/SiH_4. The variation for different points on the samples is generally less than 50nm thus the uniformity is generally good. The maximum tensile stress is achieved is 614.5MPa. Also, we can find that with the increase of stress, the refractive index will decrease, which indicates a high nitrogen composition in SiN_x.

2. Compressive stress limit:

N_2 / (N_2+He)=0%, the N_2 flow is kept at 0sccm and He flow is kept at 1300sccm. Temperature is kept at 350℃ and the chamber pressure is kept at 950mTorr. Only the

ratio of NH_3/SiH_4 is changed from 0.24 to 0.9. The stress of the experiments is shown in figure 2.

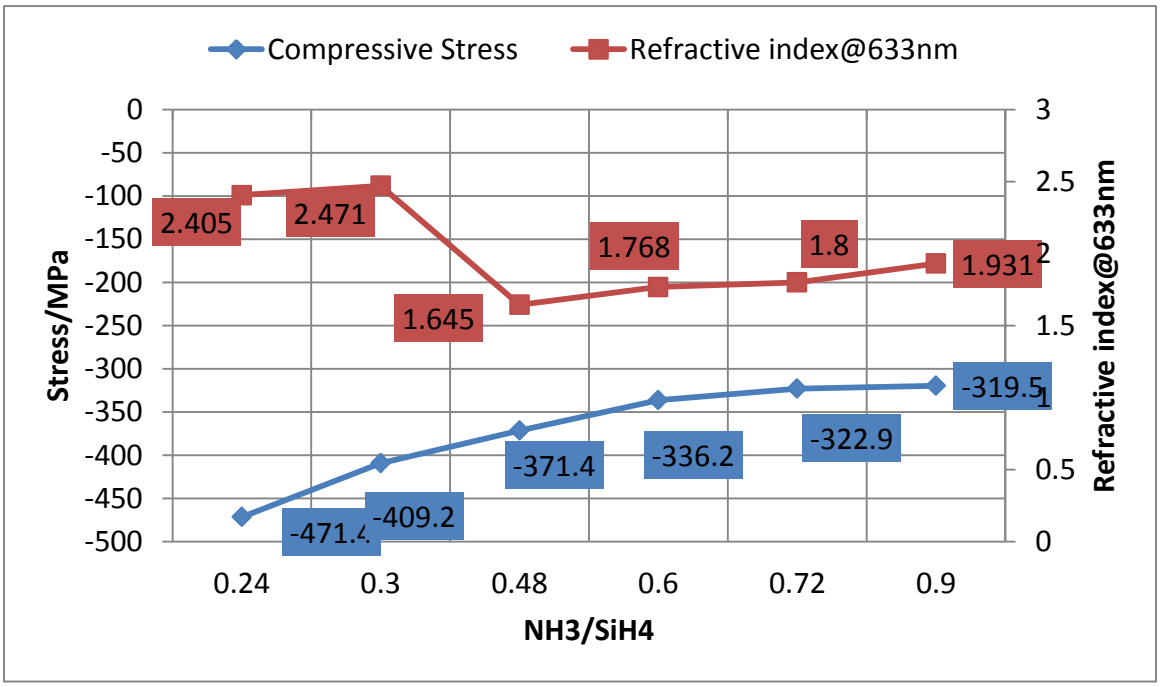

Figure 2 SiN_x Stress in compressive limit

Figure 2 shows that the stress in SiN_x in the compressive limit case is always compressive and gradually decrease as NH_3/SiH_4. But the uniformity of the samples is not good as the ones in the tensile limit case, which is due to the presence of N_2 during the deposition process serves as important factor to maintain the uniformity of the SiN_x layer. The maximum compressive stress achieved is -471.4MPa.

In this case, as we do not use any N_2 in the deposition, the uniformity is pretty bad, which will be discussed later. The modeled refractive index values also show more random changes, which indicate the poor quality of deposited SiN_x films.

3. Intermediate stress case:

N_2 /(N_2+He)=60%, the N_2 flow is kept at 600sccm and He flow is kept at 400sccm. Temperature is kept at 350℃ and the chamber pressure is kept at 950mTorr. The ratio of NH_3/SiH_4 is changed from 0 to 0.8. The stress of the experiments is shown in figure 3.

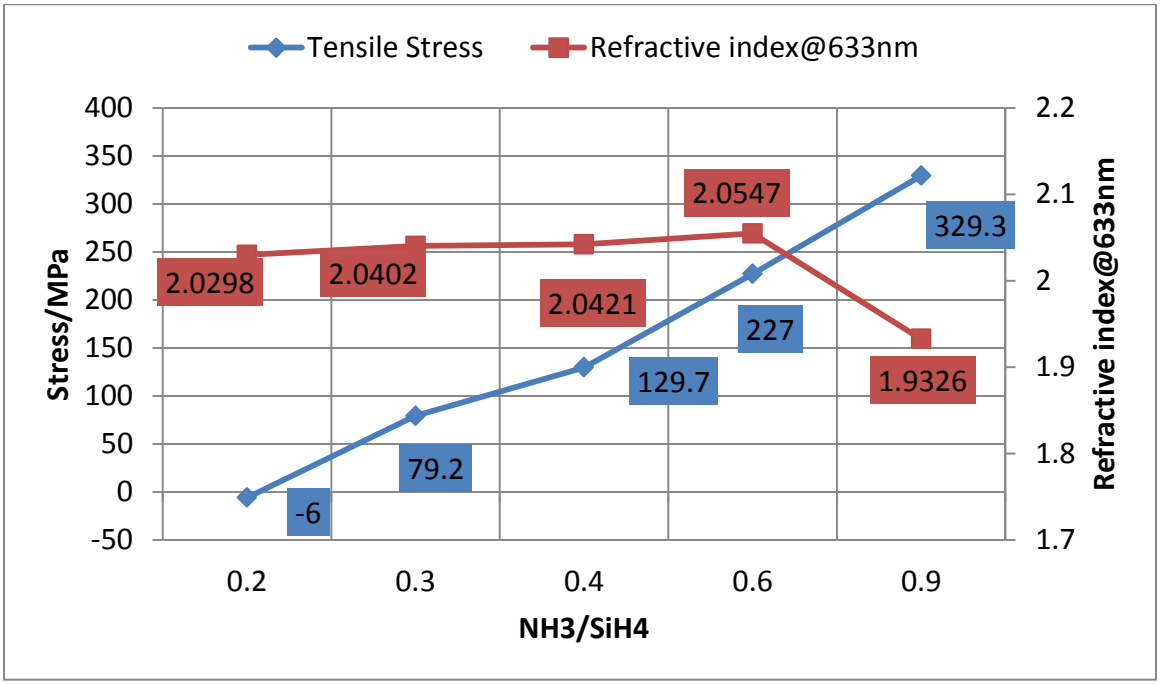

Figure 3 SiN_x Stress in intermediate case

Figure 3 shows that the stress in SiN_x in this case is cover the range both for compressive and tensile stress. When the ratio of NH_3/SiH_4 is 0.2, the SiN_x layer has almost zero residue stress, which has important application for future low stress required PECVD. Also the uniformity for these samples is good. In this case, the change of refractive index is not significant for low NH3/SiH4 ratio. However, the refractive index will decrease significantly when NH3/SiH4 ratio is larger than 0.9.

4. Deposition uniformity

In order to characterize the uniformity of SiNx films, 9 point mapping using Woollam is conducted on all samples. The results can be seen in figure 4. Y axis is the standard variation of thickness over the average thickness. X axis is the ratio of N2 / (N2 + He). We can see that if we do not use N_2, the uniformity is very bad. However, if we use more than 60% N_2, the uniformity is significantly improved.

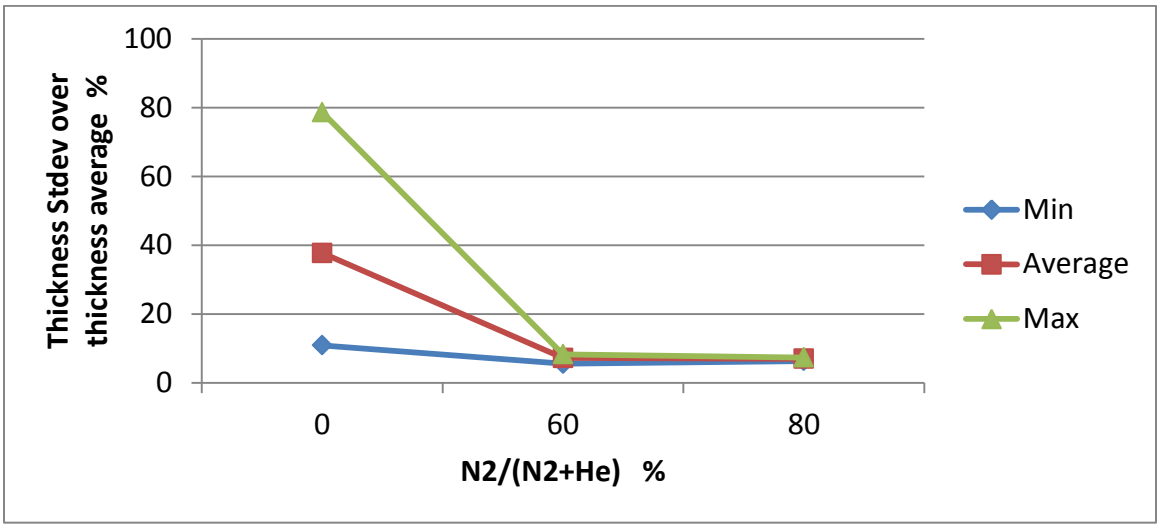

Figure 4 Uniformity of depositeyed SiN_x films. Y axis is the thickness standard variation over the average thickness. X axis is the ratio of N_2 / (N_2 + He)

ii. STS PECVD

All the experiments in STS use **pure low frequency power**.

1. Thin SiN_x deposition:

To achieve larger compressive in the SiN_x layer, the parameters for STS PECVD are mainly changed in four steps, process power, chamber pressure, ratio of NH_3/SiH_4 and deposition time.

Step 1, the chamber pressure is kept at 650mTorr, NH_3/SiH_4 at 0.84 and deposition time at 10min. Only the process power is changed for 60w, 25w and 15w. The corresponding stress and SiN_x thickness is shown in figure 5, figure 6 respectively.

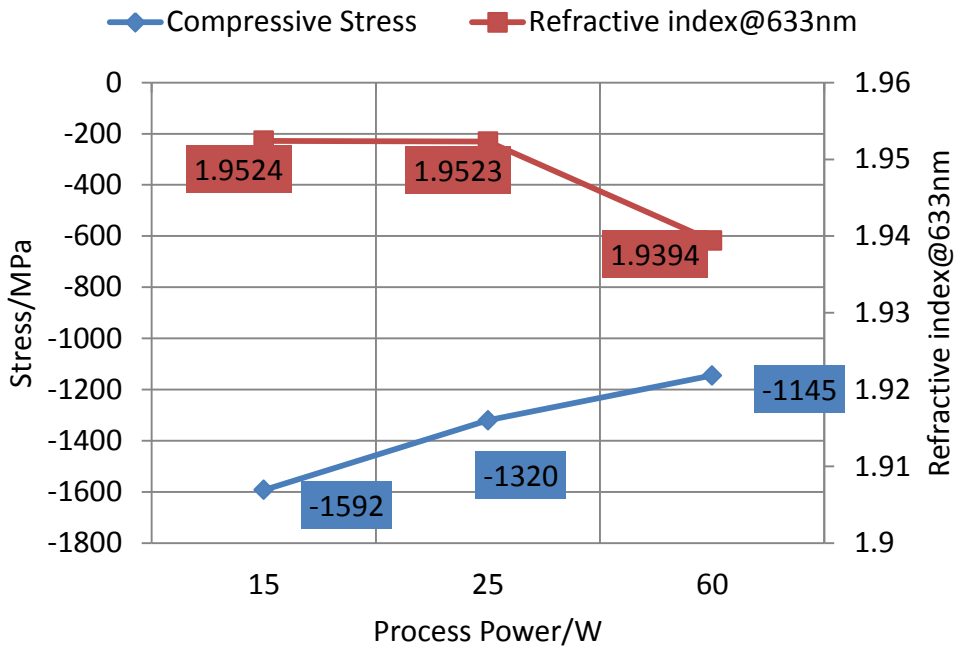

Figure 5 Process power influence on SiN_x Stress

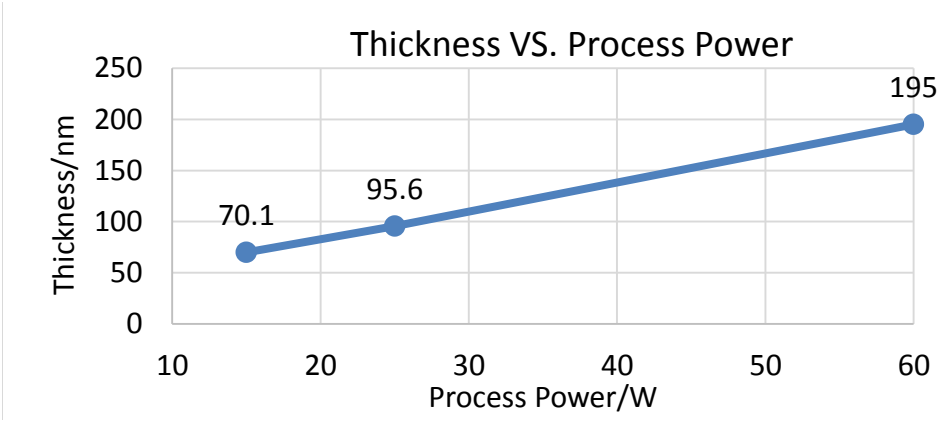

Figure 6 Process power influence on SiN_x thickness

As the figures show above, the compressive stress decreases as process power increases, also the corresponding thickness increases. The larger thickness indicates the higher growth rate, which agrees well with higher ion energy in the deposition plasma. And from the stress results, the compressive stress achieved by STS PECVD is much larger than that of CCP.

For step 2 and step 3, the chamber pressure and the ratio of NH_3/SiH_4 is changed respectively, the corresponding stress is shown in table 1 and 2.

Table 1 Pressure influence on stress

Step 2	Process power/w	Pressure/ mTorr	NH_3/SiH_4	Deposition time/min	Stress/MPa	n @ 633nm
4	25	650	0.84	10	-1320	1.9523
5	25	500	0.84	10	-1770	1.9488

Table 2 NH_3/SiH_4 influence on stress

Step 3	Process power/w	Pressure/ mTorr	NH_3/SiH_4	Deposition time/min	Stress/MPa	n @ 633nm
6	10	500	0.84	10	-1711	1.9404
7	10	500	0.38	10	**-2095**	N/A

Table 1 shows that the compressive stress in SiN_x increases from -1320MPa to -1770MPa as the chamber pressure decreases, which mainly results from longer mean free path of the ions in plasma. Further in step 3 the pressure is kept at 500mTorr and the ratio of NH_3/SiH_4 is decreased from 0.84 to 0.38, resulting to larger compressive stress from -1711MPa to -2095MPa. Thus, the largest compressive stress achieved so far is -2095MPa, in the recipe 7 of step 3.

2. Thick SiN_x deposition:

All of the SiN_x thickness on the recipes above is around or less than 100nm. To achieve thicker SiN_x around 600nm, the deposition time is prolonged to 50min and 90min, and the process power is kept at 10w, ratio of NH_3/SiH_4 is 0.37. The corresponding growth rate and stress is shown in figure 7.

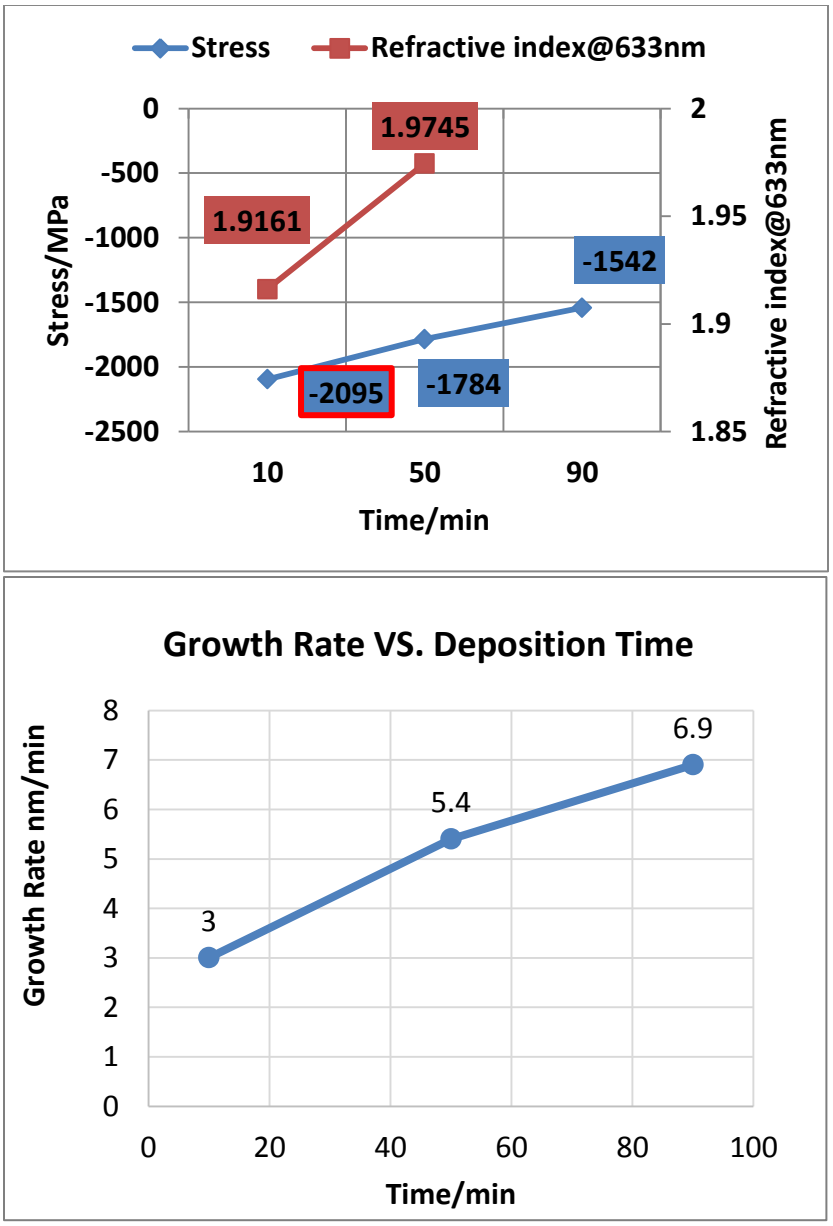

Figure 7 Time influence on stress (a) and growth rate (b)

For this case, the reduction of the compressive stress is due to the stress relaxation when the sample is heated in high temperature environment for longer time.

Furthermore, the process power is fixed at 60W and the deposition time is kept at 30min. The ratio of NH_3/SiH_4 is changed to test the influence for this parameter for long time deposition. The results are shown in figure 8.

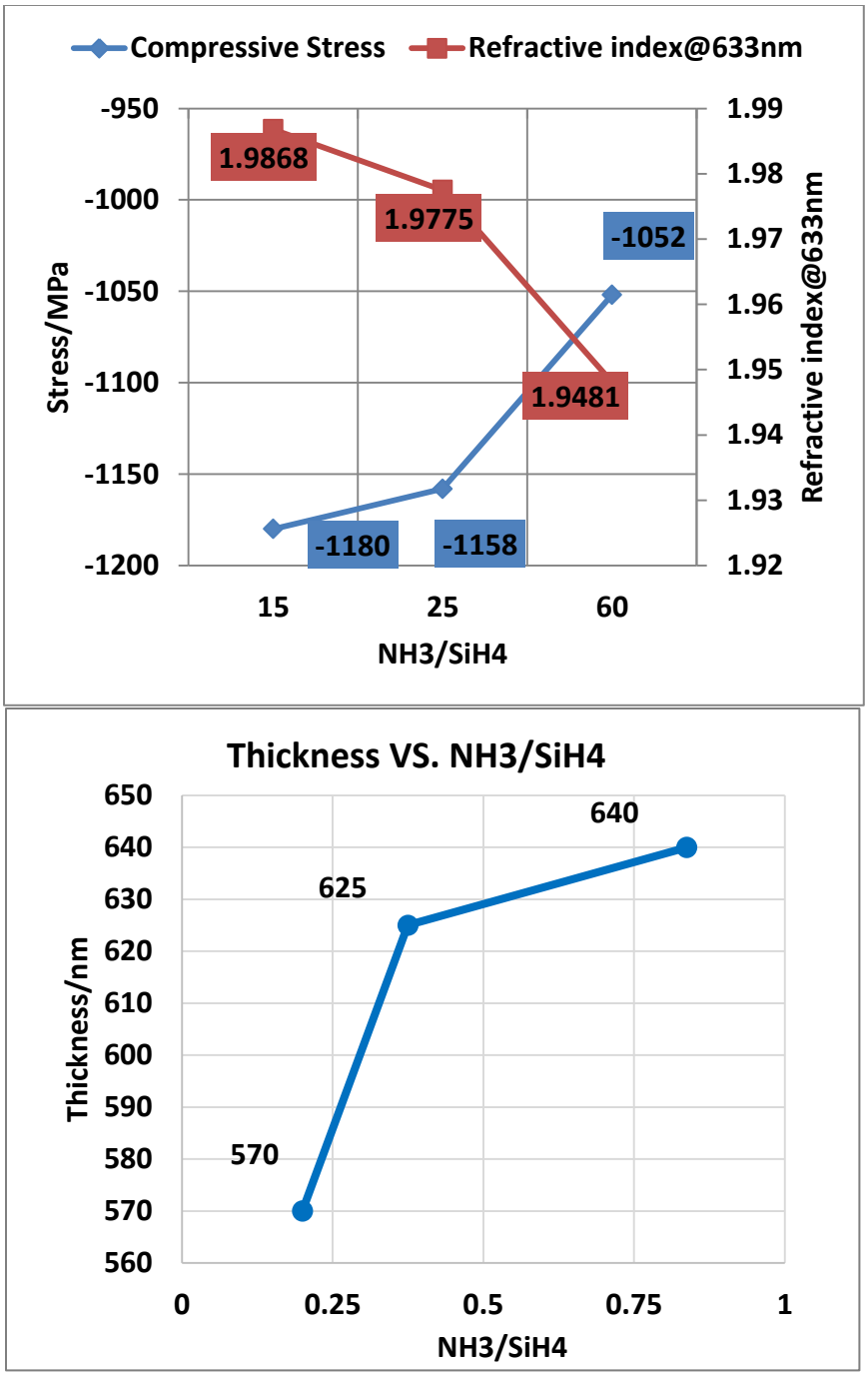

Figure 8 NH_3/SiH_4 influence on stress and growth rate for thick SiN_x

Figure 8 shows that in the long time SiN_x deposition, as the ratio of NH_3/SiH_4 changes, both the stress and the thickness does not change on a large scale. Thus this parameter has secondary effect on both the stress and growth rate of SiN_x.

c. High stress SiN_x film application

In order to evaluate the effect of stress on photonic devices, we fabricated two multi-quantum –well SiGe micro disk oscillators with CCP PECVD SiN_x films on them. The stress of one SiN_x film is 380MPa compressive stress, while the stress of the other SiN_x film is 500MPa tensile stress. The results can be seen from figure 9. The peak is shifted by ~90nm. Also, the photoluminescence intensity is almost doubled with high compressive SiN_x, which indicates that the strain has made Ge more like direct bandgap material.

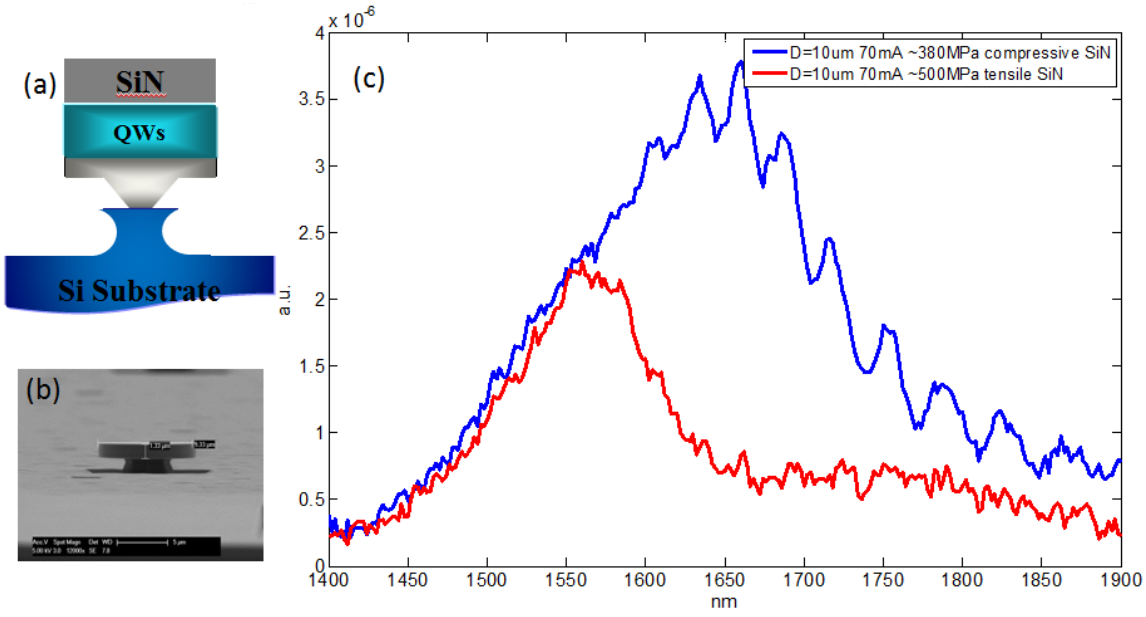

Figure 9 multi-quantum–well SiGe micro disk oscillators with CCP PECVD SiN_x films. (a) Structure schematics. (b) SEM of micro disk oscillators. (c) Photoluminescence measurement results

d. Conclusion

In this part, we have determined the stress range of CCP PECVD SiN_x, which is from -470MPa to 614MPa. Also, we have achieved a >2GPa compressive stress using STS, as in table 3. Longer deposition time will decrease the SiN_x stress due to the annealing effect. Finally, we demonstrate the importance of N_2 for the SiN_x uniformity.

Table 3 BKM (Best-Known-Method) recipe for highest compressive stress PECVD SiN_x using STS

Process power/w	Pressure/ mTorr	NH_3/SiH_4	Deposition time/min	Stress/MPa
10	500	0.38	10	-2095

III. Nanostructured SiN_x etching recipe development using nanosphere lithography technology

a. Nanosphere lithography using silica nanospheres as etching masks

In this part, we will develoe the etching recipe using PT-OX with nanosphere lithography method [11].

i. General etching process

1. SiN_x film deposition

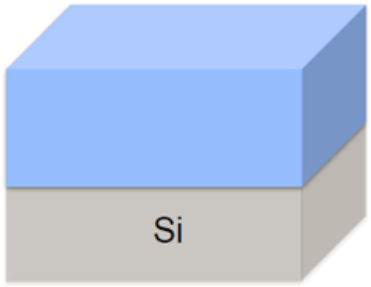

Figure 10 Film deposition

The first step is to deposite SiN_x film on Si, as in figure 10. In this report, we use CCP SiN300 recipe to deposite 900nm of SiN_x on Si.

2. Nanosphere LB coating

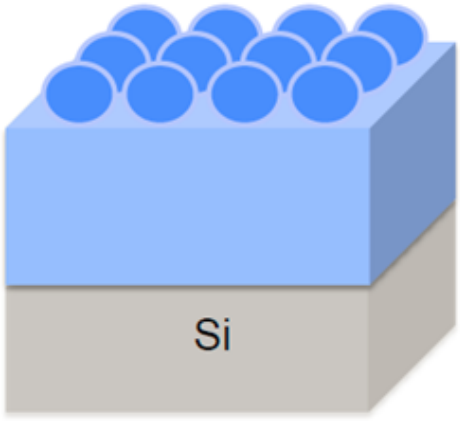

Figure 11 Nanosphere LB coating

The second step is nanosphere LB coating, as in figure 11, which will be introduced in more detail later. We use Langmuir-Blodgett (LB) Method to coat 1 mono-layer (ML) silica nanosphere as etching mask for further process, as in figure 12. In order to get high quality masks, we need to get one mono-layer of silica nanospheres on our substrate, as in figure 12(a). Otherwise we cannot get uniform nanostructures.

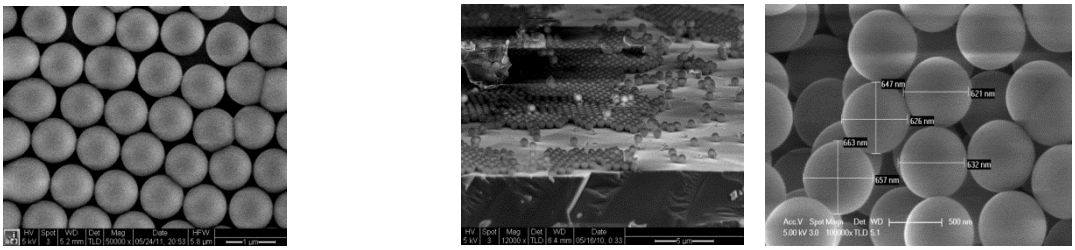

a. Good – 1ML, high uniformity b. Bad – low uniformity or multi-layers

Figure 12 Typical Cases of LB Coating

3. Reactive ion etch

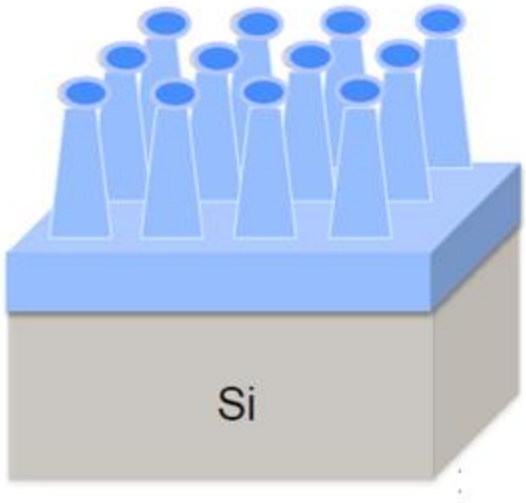

Figure 13 Reactive ion etch

The third step is reactive ion etch, which is the most sophisticated step as in figure 12. We will focus on this part later.

4. Remove nanospheres

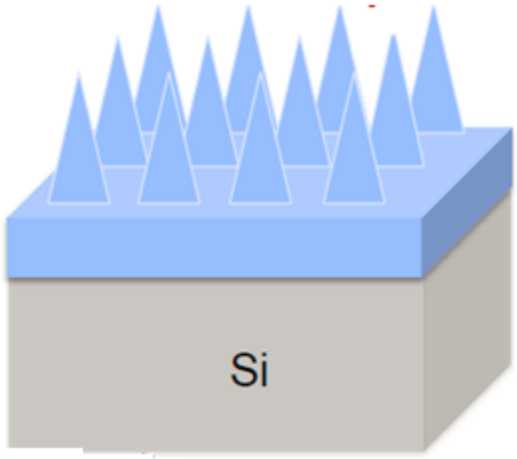

Figure 14 Remove nanospheres

The final step is to remove the remaining silica nanospheres, as in figure 13. In this project, we use 30 second dip in 50:1 HF to remove the silica nanospheres.

ii. Silica nanosphere synthesis

We need to synthesis nanospheres first. Using Stöber process [15], Tetraethyl-orthosilicate (TEOS) reacts with water to form mono-dispersed particles of silica, with ammonia as catalyst:

$$Si(OC2H5)4 + 2\ H2O \rightarrow SiO2 + 4\ C2H5OH$$

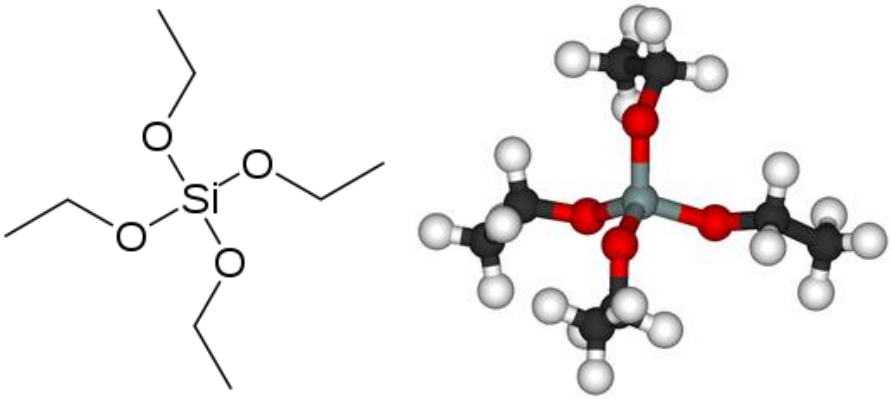

Figure 15 Tetraethyl orthosilicate (TEOS) [12]

Later, synthesized silica nanospheres need to be modified with aminopropyl methyldiethoxysilane in methanol ambient for 9 hours. This step is to terminate them with positively charged amine groups.

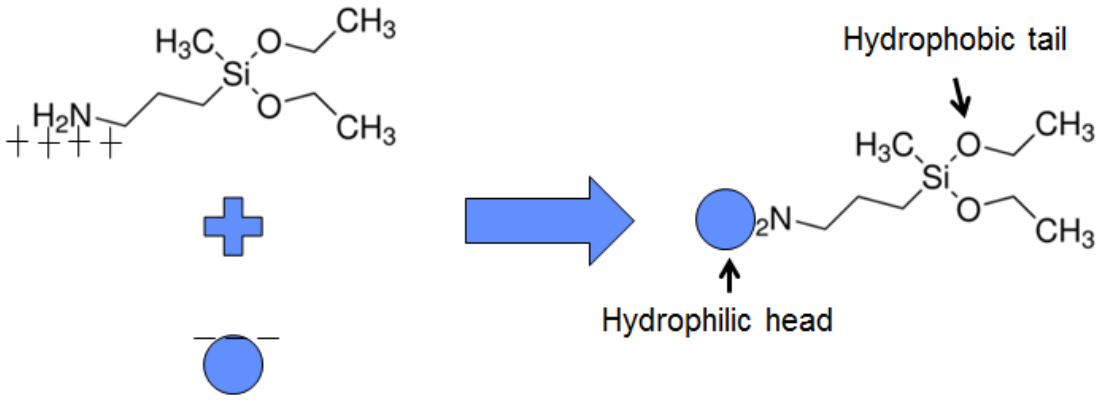

Figure 16 Modification of silica nanospheres

iii. Langmuir–Blodgett method for nanosphere coating

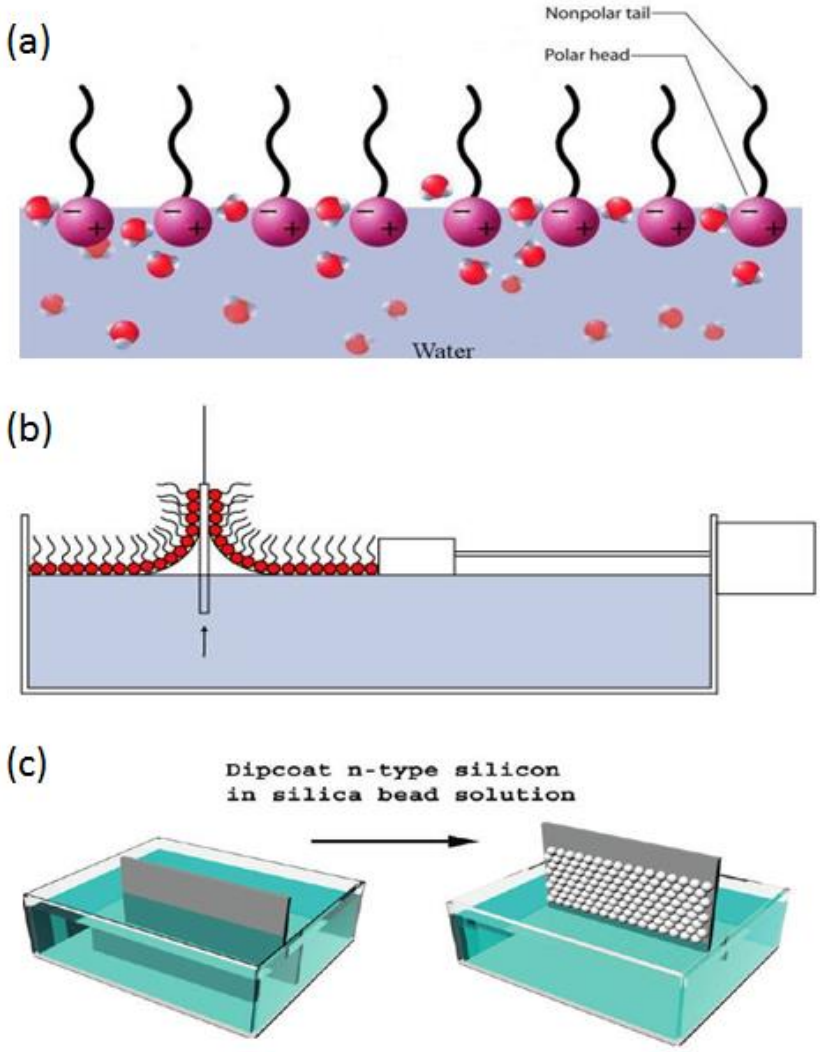

Figure 17 LB method. (a) schematic of Langmuir-Blodgett film. (b) schematic of LB coating metchod [13](c) schematic of LB coating method [14]

After modification, our silica nanospheres are with hydrophobic 'tails' and hydrophilic 'heads'. Once put onto water, amphiphilic silica nanospheres interact with air at an air–water interface. The tails will be exposed to air and the heads stay inside water, as in figure 17(a). When the nanospheres are compressed, one compact film will be formed on top of water. Then we can transfer monolayer onto a substrate by film compression, as in

figure 17(b) and 17(c). With a feedback control system using surface tension pressure of compact film as controlling parameter, we can pull up substrate from water with one mono-layer of silica nanospheres on top. The setup of LB trough at Stanford is in SMF (http://www.stanford.edu/group/snc/equipment/smf.html).

b. Nano-cone structures etching using PT-OX

i. Recipe development

Table 4 Design of experiment table

Fixed Parameters					Tuning Parameters		
Nanosphere Size (nm)	**SiN_x Thickness (nm)**	**Tempe-rature (℃)**	**ICP Power (W)**	**RF DC Bias(V)**	**Chemistry**	**Pressure (mtorr)**	**Time (s)**
600	900	10	1000	50	**CF4**	**10**	**60**
600	900	10	1000	50	**CHF3**	**20**	**120**
600	900	10	1000	50	**O2**	**30**	**240**
600	900	10	1000	50	…	**40**	**360**
600	900	10	1000	50	…	**50**	…

We want to achieve highly isotropic etching using PT-OX, as in figure 18.There many parameters to tune for PT-OX, as in table 4. After discussing with Jim Mcvittie and Jim Kruger, we decide to focus on 3 main parameters: chemistry composition, chamber pressure and etching time.

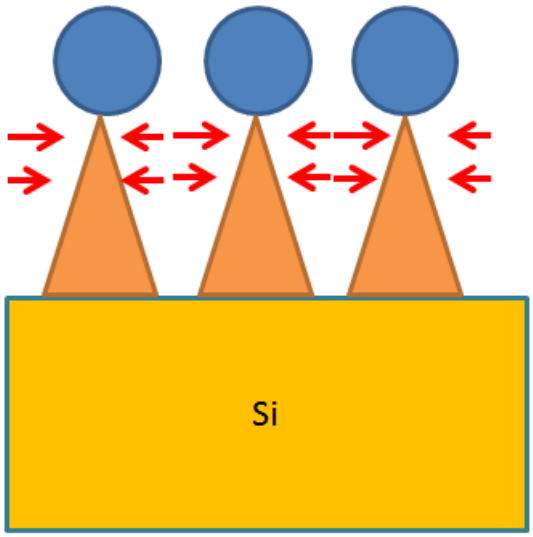

Figure 18 Highly isotropic etching

ii. Etching chemistry

Table 5 Design of experiment table for etching chemistry

Fixed parameters		Tuning parameters		
Pressure (mtorr)	**Etching Time (s)**	**Fixed O2 Flow (sccm)**	**CF4 Flow (sccm)**	**CHF3 Flow (sccm)**
30	240	5	45	5
30	240	5	35	15
30	240	5	25	25
30	240	5	15	35
30	240	5	5	45

One typical set of parameter design can be seen in table 5. We fixed the chamber pressure to be 30 mtorr and the etching time to be 240s. We also fix the O2 flow to be 5sscm and CF4+CHF3 flow to be 50sccm. Then we varied CHF3 percentage from 5% to 95%. The etching results can be seen in figure 19. We can see that with the increase of CHF3 percentage, the etching will be more anisotropic and the etching rate will

also be decreased, which is not favored. Therefore, for highly isotropic etching, we need to have minimum amount of CHF3, which is 0.

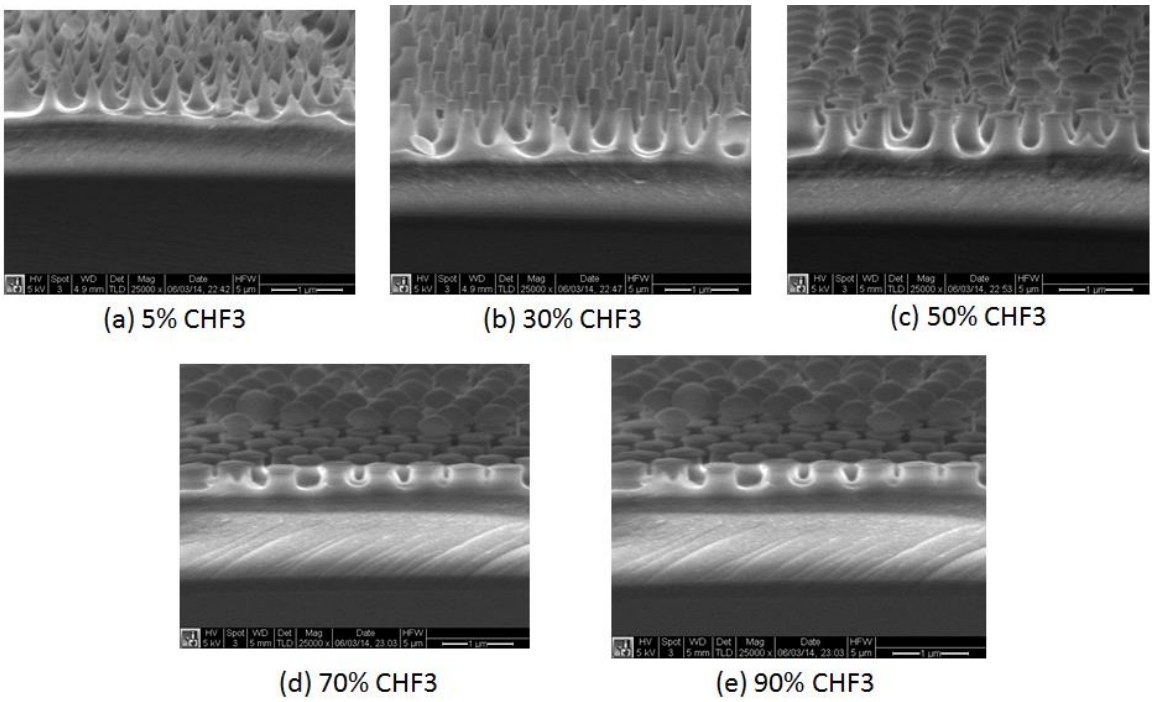

Figure 19 SEM images showing effect of different etching chemistry

iii. Etching pressure

Table 6 Design of experiment table for etching pressure

Fixed parameters			Tuning parameters
Etching Time (s)	**Fixed O2 Flow (sccm)**	**CF4 Flow (sccm)**	**Pressure (mtorr)**
120	5	50	**10**
120	5	50	**20**
240	5	50	**30**
240	5	50	**40**
240	5	50	**50**

One typical set of parameter design can be seen in table 6. From the conclusion of previous section, we should have 0 CHF3. So we only have 5sccm of O2 flow of 50sccm of CF4 flow. For etching time, as the etching rate is much higher in low pressure case, we choose it to be 120s for 20mtorr and 10mtorr cases. For 30mtorr, 40mtorr and 50mtorr cases, we set it to be 240s. From the results in figure 20, we can see that with higher chamber pressure, the etching will be more isotropic and the etching rate will be lower. That is due to the more scattering of ions and the decrease of mean free path. Therefore, we want to have high chamber pressure. However, we also find it that if we increase the chamber pressure to be larger than 50mtorr, the chamber plasma may not be stable under 50V DC bias. That might result from the high plasma density at high chamber pressure. As a result, finally we choose the chamber pressure to be 50mtorr.

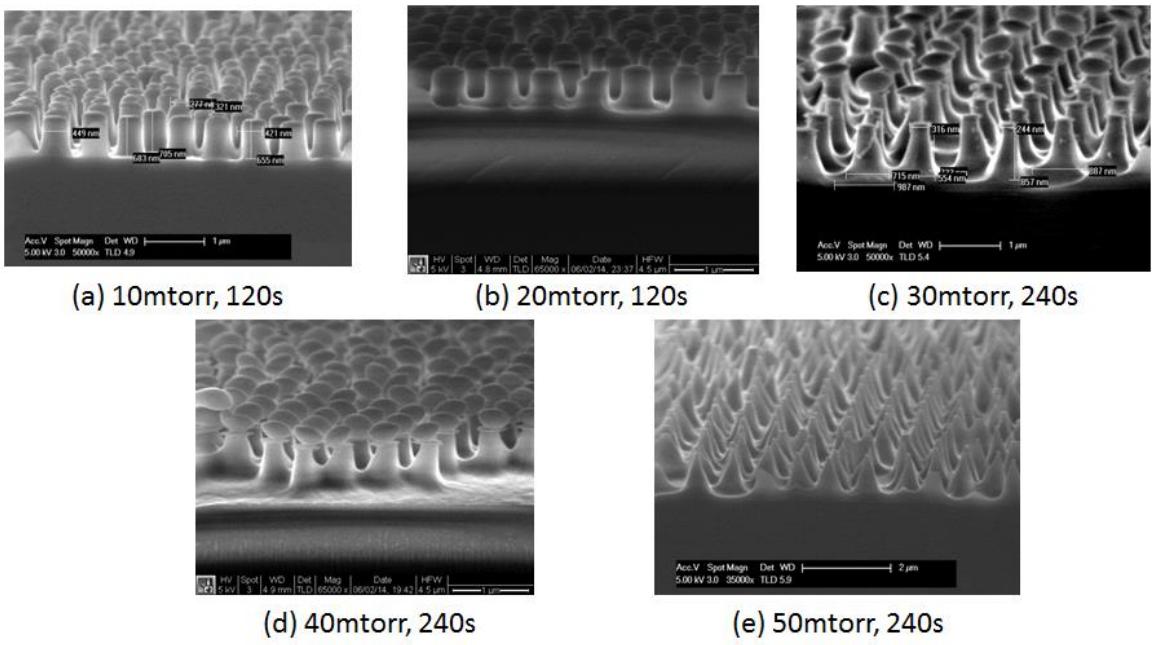

Figure 20 SEM images showing effect of etching pressure

iv. Etching time

Table 7 Design of experiment table for etching time

Fixed parameters			Tuning parameters
Pressure (mtorr)	**Fixed O2 Flow (sccm)**	**CF4 Flow (sccm)**	**Etching Time (s)**
50	5	50	**60**
50	5	50	**120**
50	5	50	**240**
50	5	50	**360**

One typical set of parameter design can be seen in table 7. We fixed the chamber pressure to be 50mtorr, O2 flow to be 5sccm and CF4 flow to be 50sccm. Etching time need to be carefully tuned, as over-etch and under-etch are both not favored in nanostructure etching. To get the best cone shape, the etching time should be carefully controlled, as in figure 21. In figure 21(a) and (b), we can see the etching time is not enough. Figure 21(c) shows favored nano-cone structures. However, if we further etch our samples, as in figure 21(d), the over-etch will destroy all of our nanostructures. We need to be super careful with this.

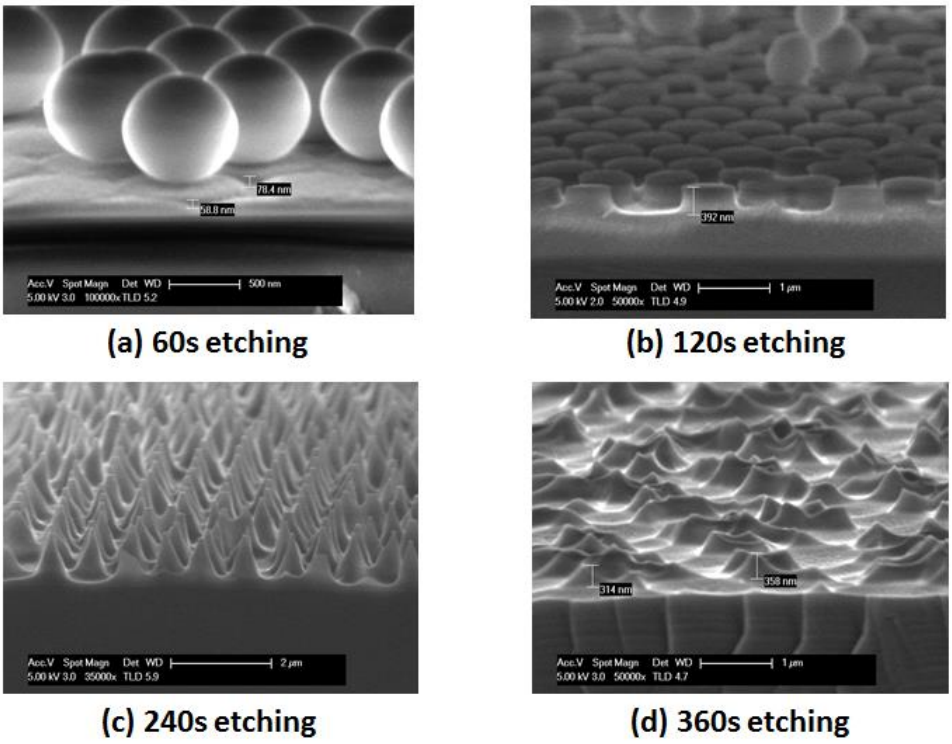

Figure 21 SEM images showing effect of etching time

c. BKM recipe and anti-reflection result

Finally, our BKM recipe is determined as in table 8. The etched structure is as in figure 22. Reflection measurements were performed using a standard integrating sphere system as in figure 23 [16]. Incident light entered the sphere through a small port and illuminates the sample mounted at the center of the sphere. The reflected light was scattered uniformly by the interior sphere wall. A silicon detector mounted at the back of the sphere produced a photocurrent from all the reflected photons. The measured results of normalized reflection under different incident light angles for our nanostructured SiN_x on Si and its planar Si control sample are shown in figure 22. The reflection has been suppressed from ~30% to ~10% from 0 to 60 degrees, showing a wide-angle anti-reflection effect.

Table 8 BKM Etching Recipe

Pressure (mtorr)	Fixed O2 Flow (sccm)	CF4 Flow (sccm)	Etching Time (s)
50	**5**	**50**	**240**

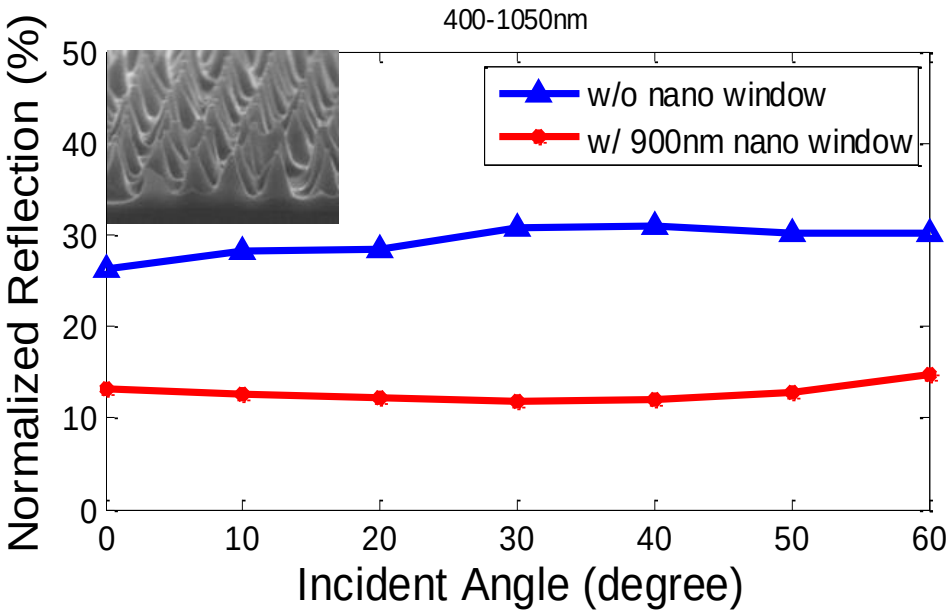

Figure 22 Reflection measurement

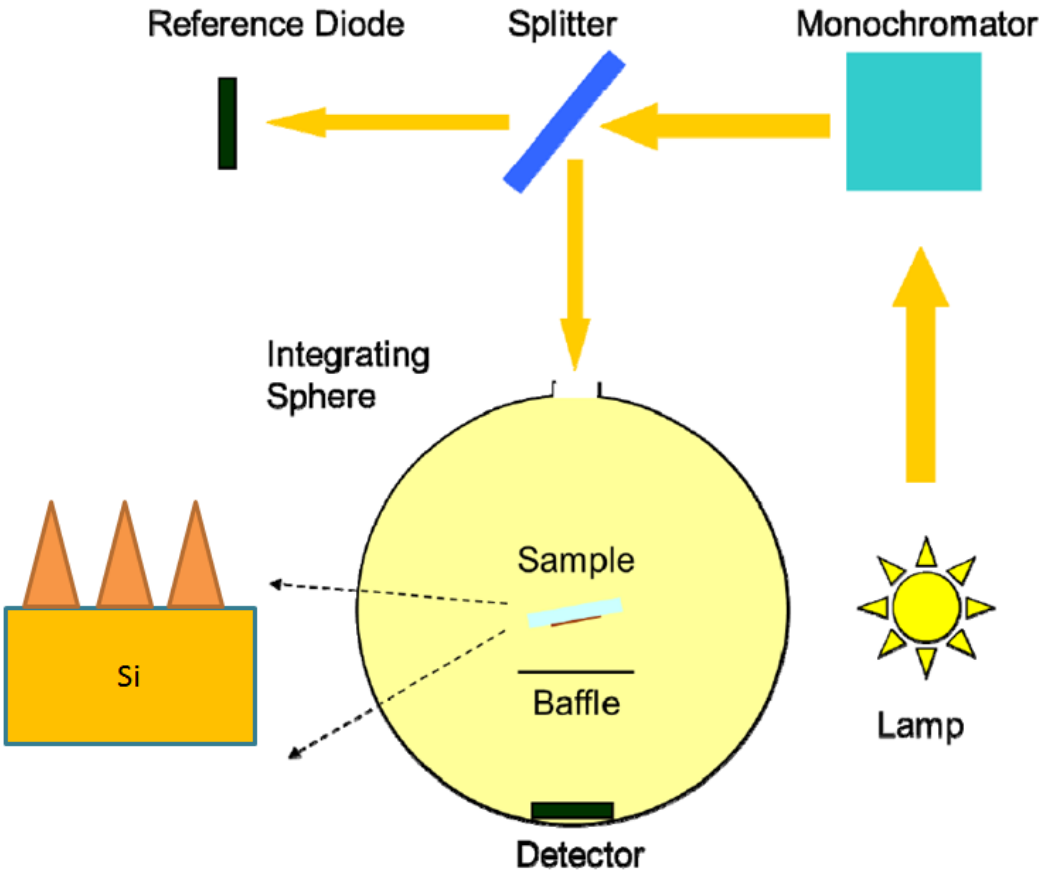

Figure 23 Reflection measurement setup [16]

IV. Summary and future work

In summary, we achieved >2GPa stress in PECVD SiN_x films on Si. We also successfully achieved highly isotropic nanostructure etching using PT-OX. A systematic study of SiN_x PECVD and RIE etching recipe development is also performed.

In the future, we would like to continue this work in the following fields:

1. **Determine the Young's modulus for SiN_x films**

   In this work, we mainly focus on the stress test of SiN_x films. However, if we want to determine the strain distribution in the underlying Si or SiGe samples, we need to know the Young's modulus of our films. In the future, we would like to

measure and model the Young's modulus. Such work will also be helpful for MEMS and photonics people in SNF.

2. **Continue the study of nanostructure etching**

   We have shown a good guidance for nanostructure etching recipe development. In the future, we would like to do more modeling and simulation work to determine the best SiN_x nanostructures for different applications and then develop etching recipes for them.

3. **More dielectric materials!**

   In this EE412 project, we focus on SiN_x. However, there are more interesting dielectric/amorphous materials available in SNF, including a-Si, SiO_x, SiC and etc. If possible, we would also like to develop different PECVD and RIE etching recipes for those materials.

V. Acknowledgement

First, we would like to express our most sincere thanks to the EE412 teaching team: Prof. Roger Howe, Dr. Mary Tang, Dr. Michelle Rincon and Dr. J Provine. I still remembered when they encouraged me to find another setup of LB trough when I disappointedly found that the one in SMF was down. Then I tried to find one working LB trough in Prof. Melosh's group. Without their encouragement, we may not be able to demonstrate the nanostructure etching part (that may also kill Jieyang and Li's project…).

Send, we would like to thank our mentors, Dr. Jim Mcvittie and Prof. Harris. Without their guidance, we will be totally lost in the ocean of recipe development.

Finally, we would like to thank the SNF staff members, including Uli, Nancy, Maurice, James, Elmere, Mahnaz and Jim. Thank you so much for your support to make all the tools running well! Hopefully you will not just treat us as trouble-makers!

References:

[1] Aberle, Armin G. "Overview on SiN surface passivation of crystalline silicon solar cells." Solar Energy materials and solar cells 65.1 (2001): 239-248.

[2] Nagel, Henning, Armin G. Aberle, and Rudolf Hezel. "Optimised antireflection coatings for planar silicon solar cells using remote PECVD silicon nitride and porous silicon dioxide." Progress in Photovoltaics: Research and Applications7.4 (1999): 245-260.

[3] Nam, Donguk, et al. "Strained germanium thin film membrane on silicon substrate for optoelectronics." Optics express 19.27 (2011): 25866-25872.

[4] Sawada, Toru, et al. "High-efficiency a-Si/c-Si heterojunction solar cell."Photovoltaic Energy Conversion, 1994., Conference Record of the Twenty Fourth. IEEE Photovoltaic Specialists Conference-1994, 1994 IEEE First World Conference on. Vol. 2. IEEE, 1994.

[5] Stress control of Si-Based PECVD Dielectrics, K. D Mackenzie, D. J. Johnson, 207th Electrochemical Society Meeting, Quebec City Canada, May 2005

[6] Schmidt, Jan, Mark Kerr, and Andres Cuevas. "Surface passivation of silicon solar cells using plasma-enhanced chemical-vapour-deposited SiN films and thin thermal SiO2/plasma SiN stacks." Semiconductor science and technology16.3 (2001): 164.

[7] Kim, D. S., et al. "Refractive index properties of SiN thin films and fabrication of SiN optical waveguide." Journal of electroceramics 17.2-4 (2006): 315-318.

[8] Chen, Y., et al. “Nanostructured dielectric layer – a new approach to design nanostructured solar cells”, to appear on PVSC 40 (2014)

[9] Kastenmeier, B. E. E., et al. "Chemical dry etching of silicon nitride and silicon dioxide using CF4/O2/N2 gas mixtures." Journal of Vacuum Science & Technology A 14.5 (1996): 2802-2813.

[10] Reyes-Betanzo, C., et al. "Silicon nitride etching in high-and low-density plasmas using SF 6/O 2/N 2 mixtures." Journal of Vacuum Science & Technology A: Vacuum, Surfaces, and Films 21.2 (2003): 461-469.

[11] C.-M. Hsu, et al, "Wafer-scale silicon nanopillars and nanocones by Langmuir–Blodgett assembly and etching," Applied Physics Letters, vol. 93, pp. 133109-133109-3, 2008.

[12] http://en.wikipedia.org/wiki/Tetraethyl_orthosilicate

[13] http://en.wikipedia.org/wiki/Langmuir%E2%80%93Blodgett_film

[14] S. Jeong, L. Hu, H. R. Lee, E. Garnett, J. W. Choi and Y. Cui, "Fast and Scalable Printing of Large Area Monolayer Nanoparticles for Nanotexturing Applications," *Nano Letters*, 10, 2989-2994(2010)

[15] B. O. Dabbousi, et al, "Langmuir-Blodgett Manipulation of Size-Selected Cdse Nanocrystallites," Chemistry of Materials, vol. 6, pp. 216-219, 1994

[16] Dong Liang ; Yangsen Kang ; Yijie Huo ; Ken Xinze Wang ; Anjia Gu ; Meiyueh Tan ; Zongfu Yu ; Shuang Li ; Jieyang Jia ; Xinyu Bao ; Shuang Wang ; Yan Yao ; Shanhui Fan ; Yi Cui ; James Harris; GaAs thin film nanostructure arrays for III-V solar cell applications. Proc. SPIE 8269, Photonic and Phononic Properties of Engineered Nanostructures II, 82692M (February 9, 2012); doi:10.1117/12.909743.